Óbuda University – Doctorate School on Materials Science and Technologies Obuda University, Hungary

Testing in Semi-Solid State

by

Kawan M. Abdulrahman

PhD Student

kawan.abdulrahman@bgk.uni-obuda.hu

Supervisors by :

Prof. Dr.Réger Mihály and Dr. Viktor Gonda

Seventh semester

15/06/2021

Outline

- ✓ Background of Dendritic and Non-Dendritic Structure
- ✓ Microstructures in Semisolid Metalworking
- ✓ Why Semi - Solid Methods?
- ✓ Semi-Solid Process Window
- ✓ Background of Semi-Solid
- ✓Aluminum Alloys
- ✓Previous work
- ✓Results and Conclusion
- ✓Activity of all Semesters
- ✓Future Research Plan

Dendritic and Non-Dendritic Structure

What is dendritic structure?

Grain structure of ingot

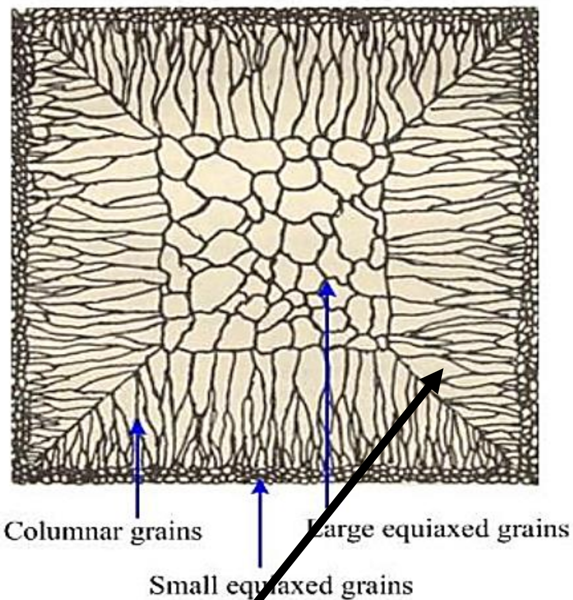

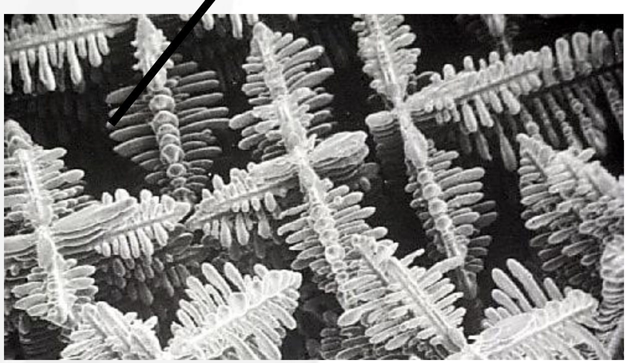

Dendritic structure of material

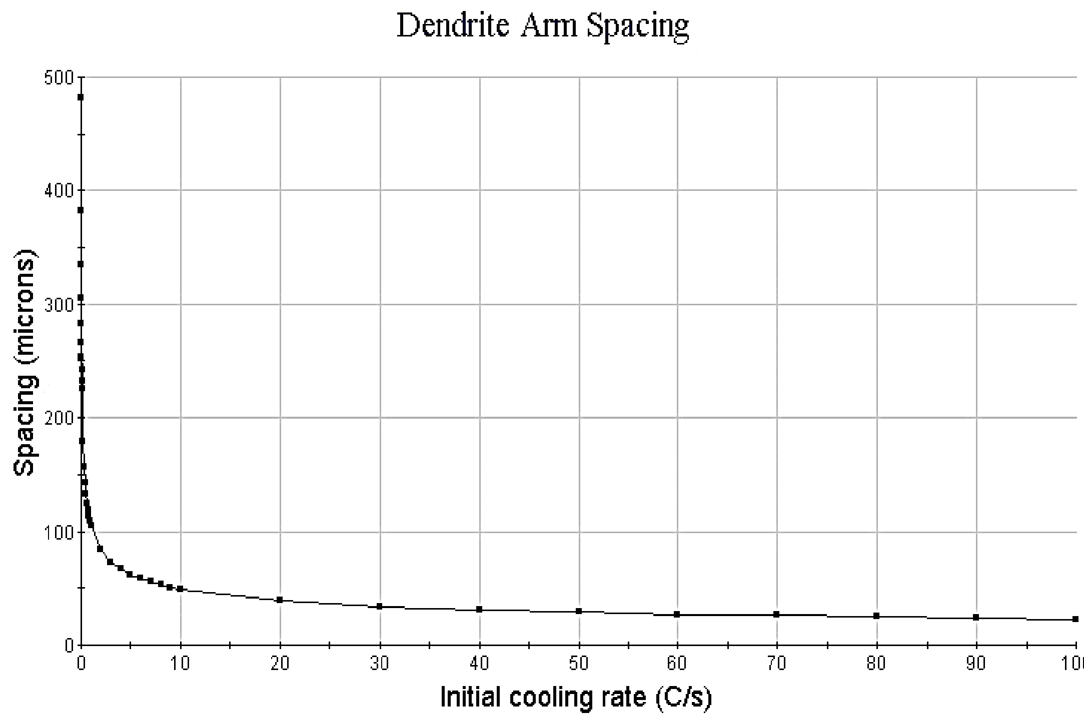

Figure 1. Dendritic arm spacing

Dendritic and Non-Dendritic Structure

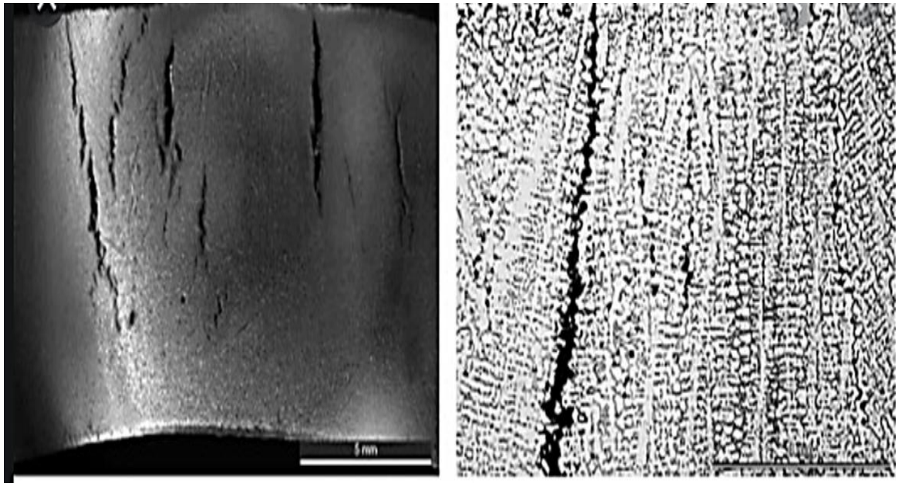

Figure 2. Failure Arm Dendritic structure

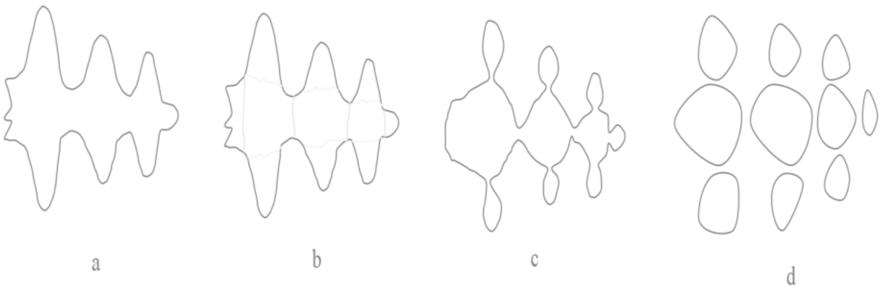

Dendritic arm structure **Spheroidal shape**

(a and b) The shear stresses change the shape of the solid particles from dendritic (c and d) to globular

Microstructural changes

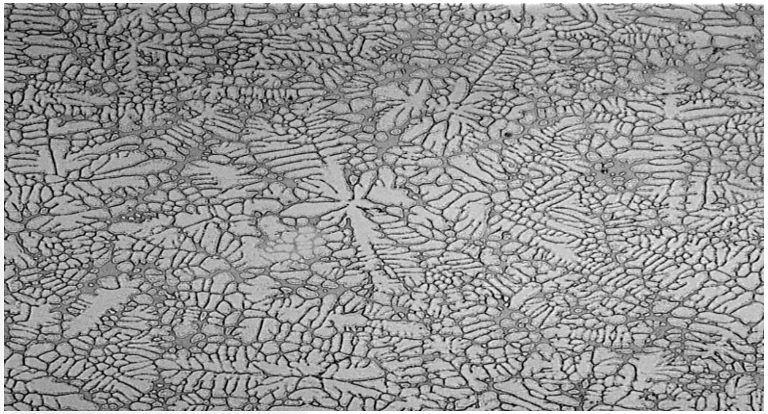

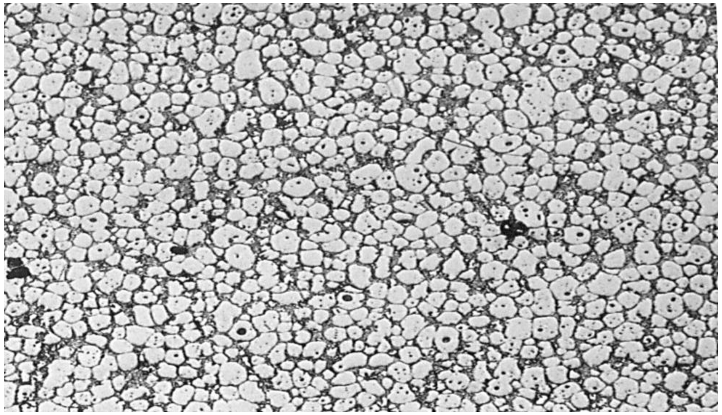

Figure 3. a.Typical Dendritic Microstructure   *b.Typical Non Dendritic Microstructure*

Microstructures in Semisolid Metalworking

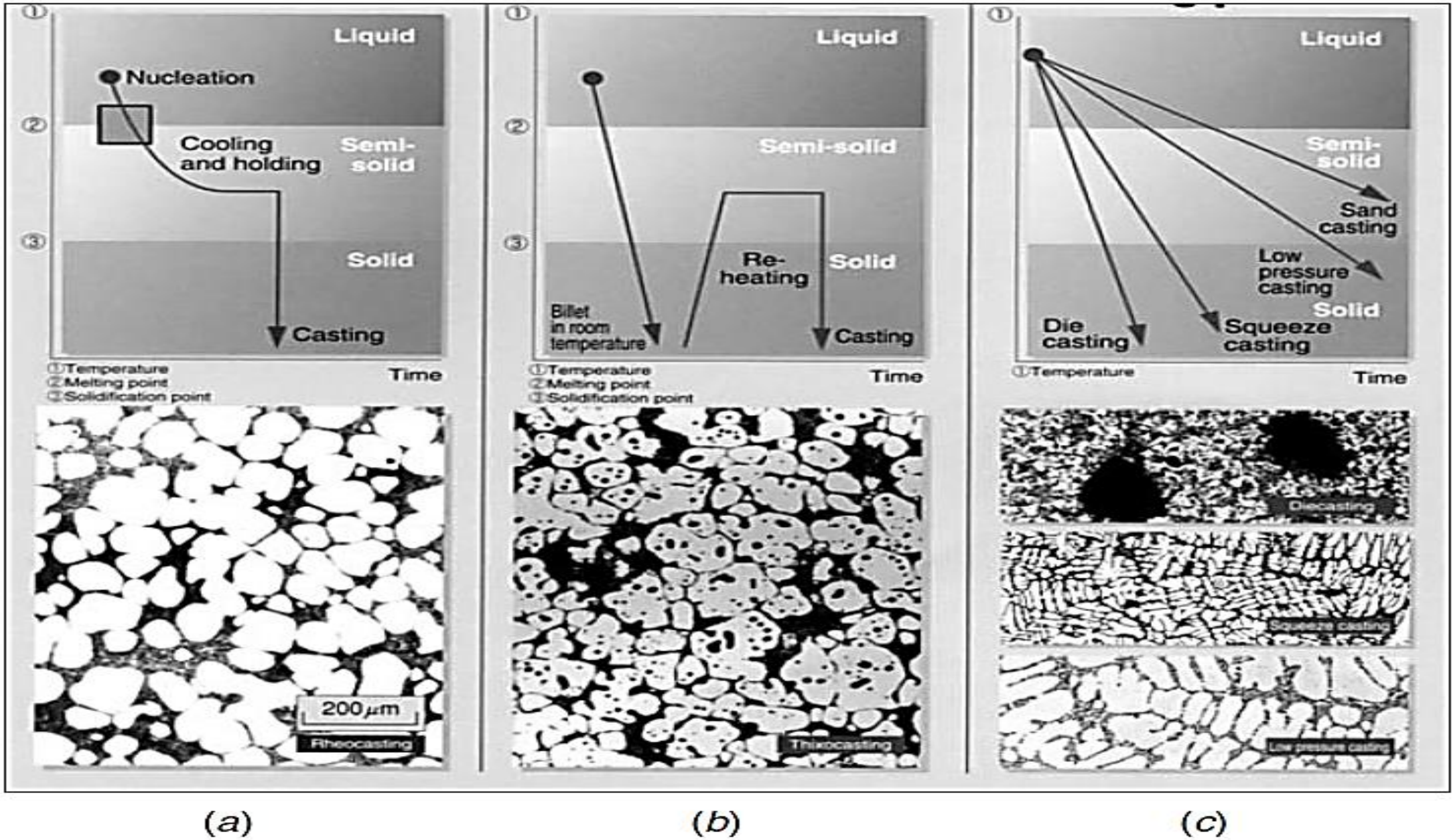

Figure4. Process comparison between (a) direct semi-solid metalworking, (b) indirect semi-solid metalworking, and (c) conventional casting processes

Why Semi - Solid Methods?

Technical and economical comparaison to other common forming techniques :

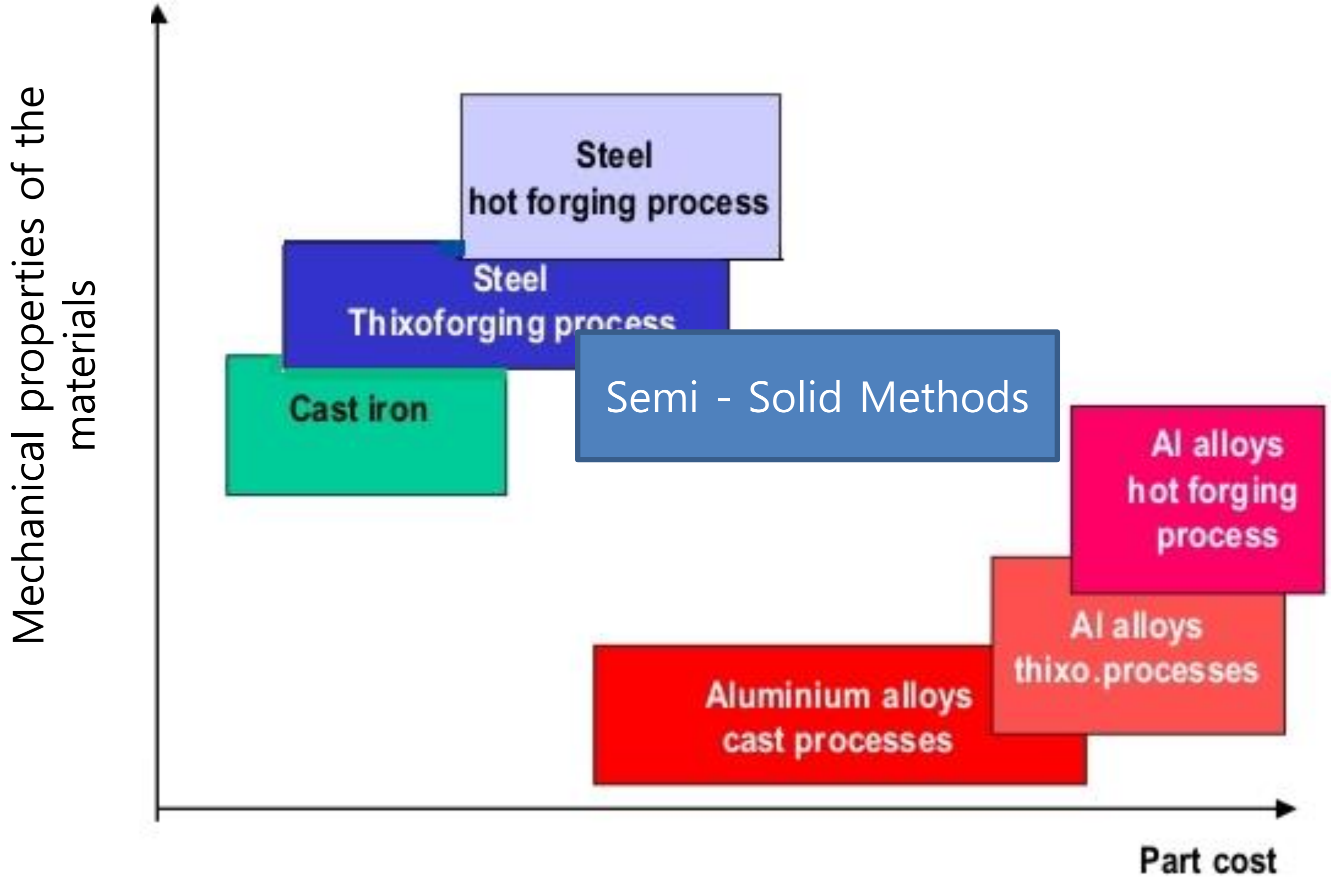

Future 5. Semi - Solid Methods alloys will be placed somewhere here in future assuming a well established process

What is Semi-Solid State?

Semi-Solid Process Window

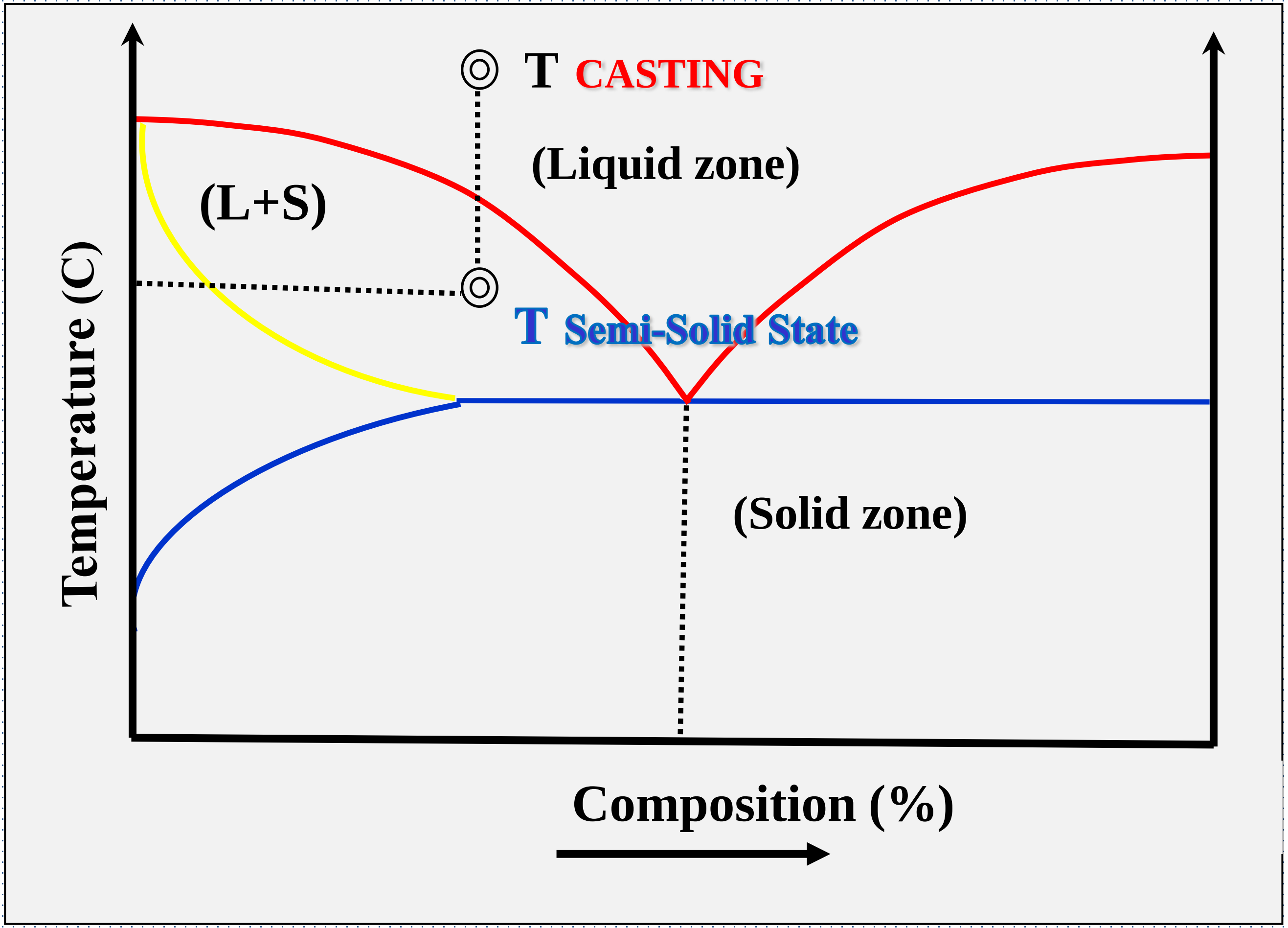

Figure 6. Phase diagram

Background of Semi-Solid

Semi - Solid Methods

1. Semi-Solid Rheocasting (SSR) process
2. Magneto Hydrodynamic (MHD) Method vertical, horizontal, and helical
3. Cooling Slope Method (CS)
4. SSR with CS techniques (SS + CS)

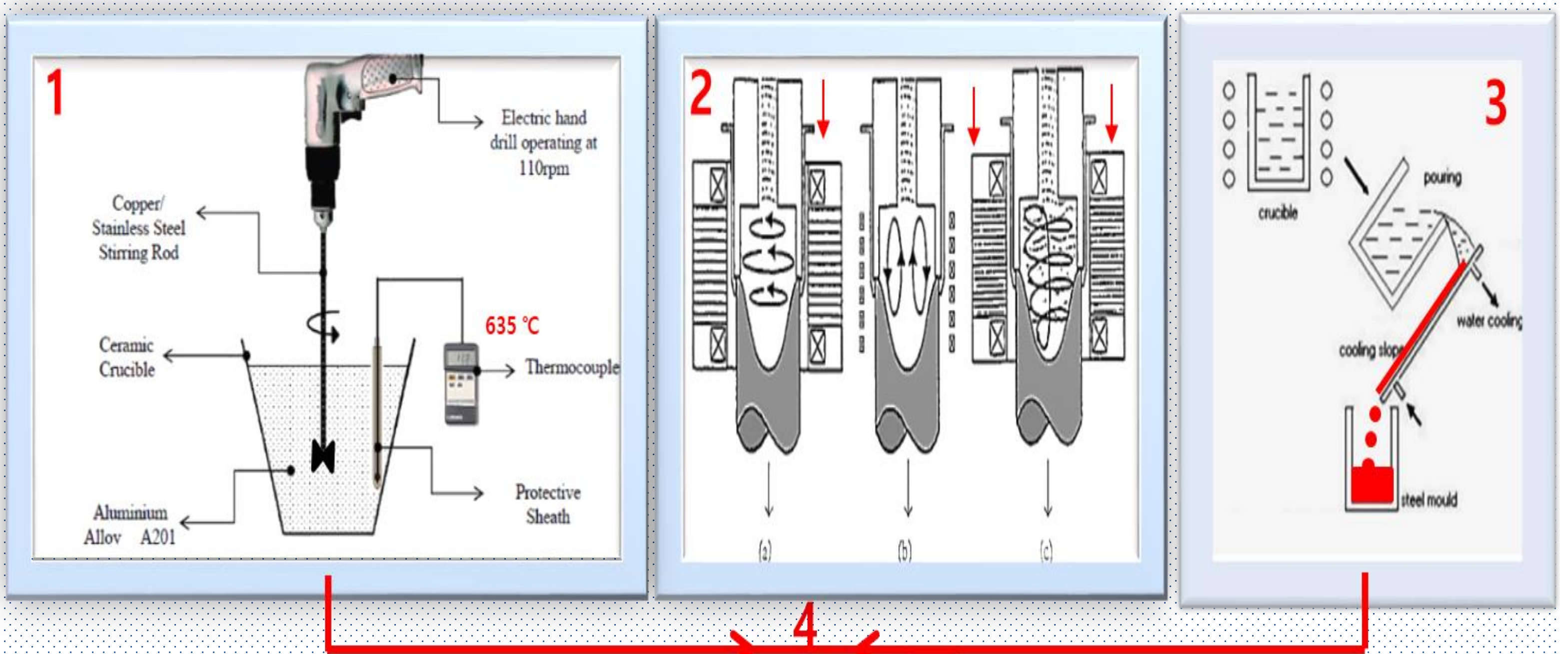

Figure 7. Semi - Solid Methods

Aluminum Alloys

Al alloys	Wt%	Cu	Mn	Mg	Si	Fe	Ti	Ag	Ca	Cr	Zn
EN AW 2011	93.97	4.7	0.31	0.28	0.10	0.05	0.21	0.59	-	-	-
EN 6063-T6	98.676	0.002	0. 1	0.45	0.32	0.26	0.1	-	0.001	0.25	0.001
EN AW 6082	98.07	0.1	0.4	0.5	0.33	0.25	0.1	-	-	0.25	0.2

Table 1. Chemical composition of all aluminium alloys

Previous work

Microstructure Results

Aluminum EN AW 2011 alloy

Dendritic structure

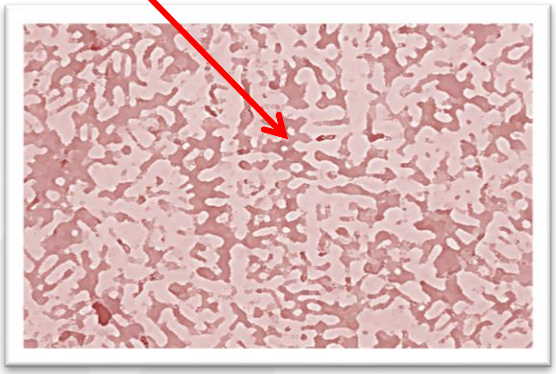

Dendritic Microstructure

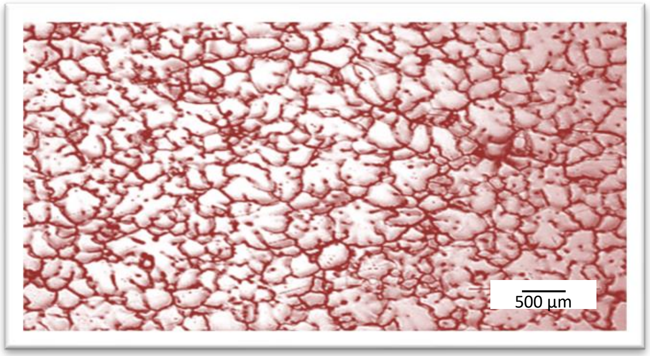

CS Micrograph

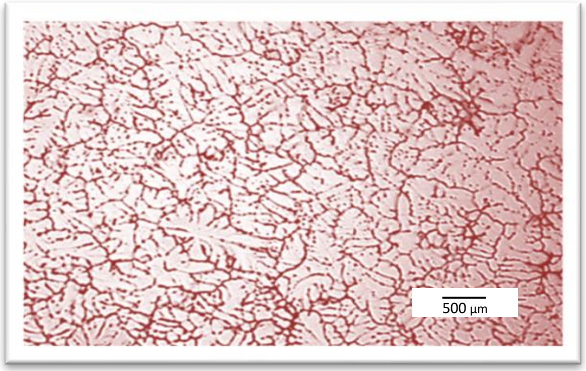

MHD Micrograph

Spheroidal shape

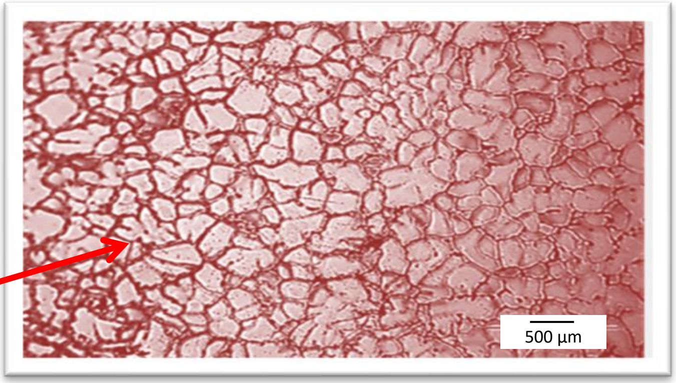

SSR Micrograph

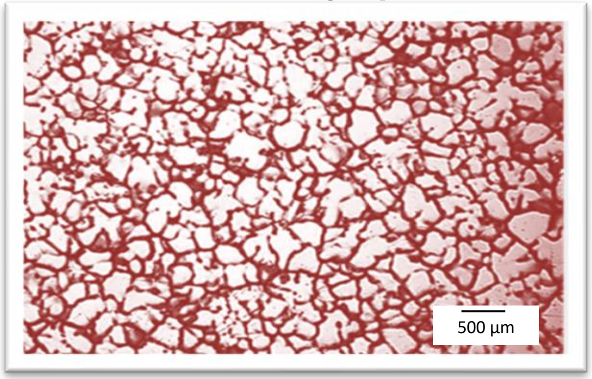

SSR + CS Micrograph

Figure 8. Microstructure of all Semi - Solid Methods

Previous work

Microstructure Results

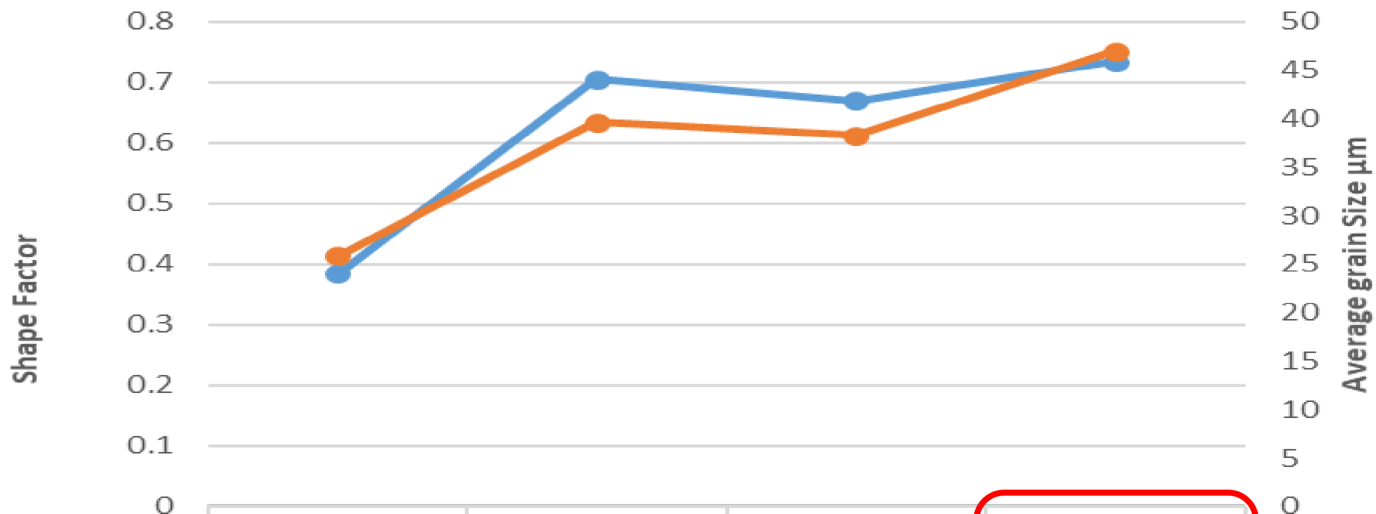

	MHD	CS	SSR + CS	SSR
Shape Factor	0.385	0.705	0.67	0.735
Grain Size µm	25.85	39.64	38.32	46.95

Figure 9. Shape Factor and Grain size of variance types of Alloy A201

Shape Factor (*Solid Fraction*) **= 4 π A/ P^2**

P = the average perimeter.

A = the average area of the grains

S. F. = value should be between 0.6 and 1.0

Previous work

Mechanical Properties Results

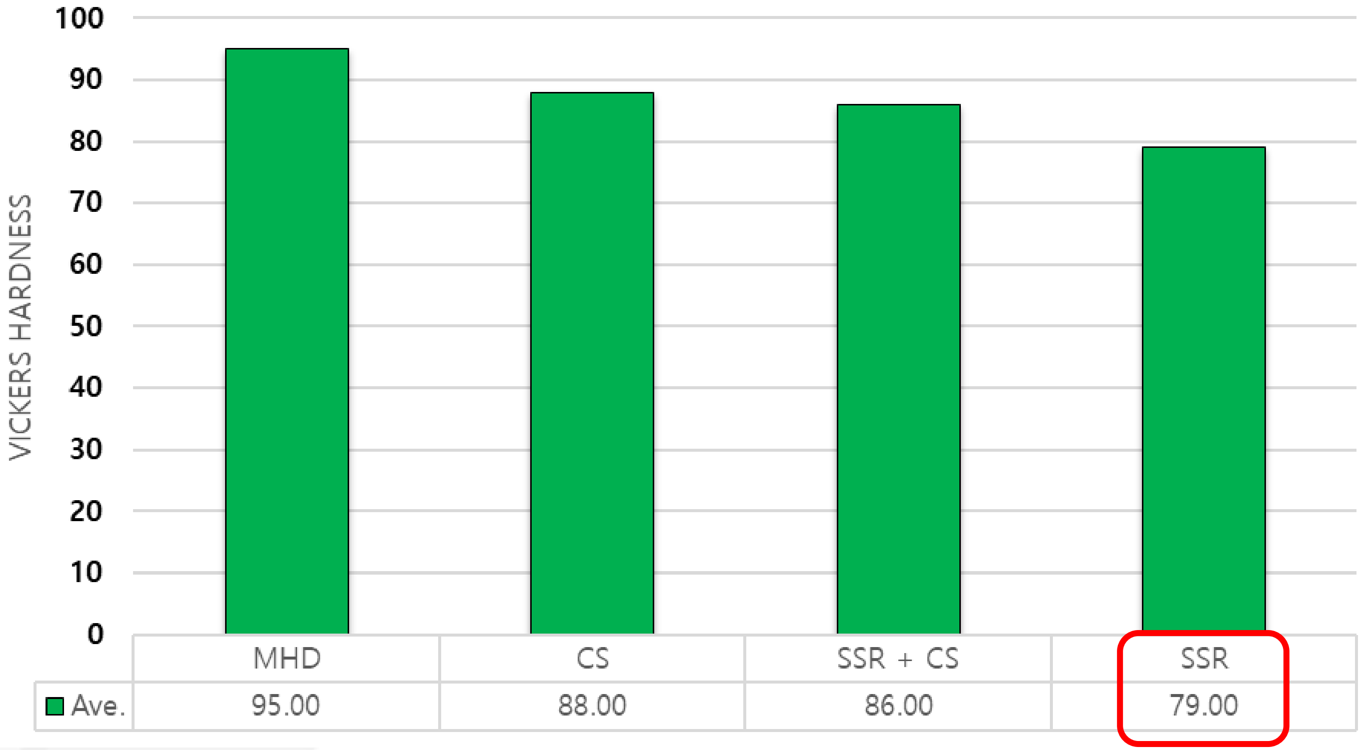

Figure 10. Vickers Hardness of all Methods

Previous work

- **Tensile test and Compression test**

Aluminum EN 6063-T6 Extrusions alloy

Aluminum type`	Yield Strength (σy) MPa	Ultimate Tensile Stress (UTS) MPa	% Strain
Aluminium Extrusions	215	241	0.080
Aluminium Rheocasting	290	340	0.110

Table 2. Results of the stress-strain curve of the two-sample alloy.

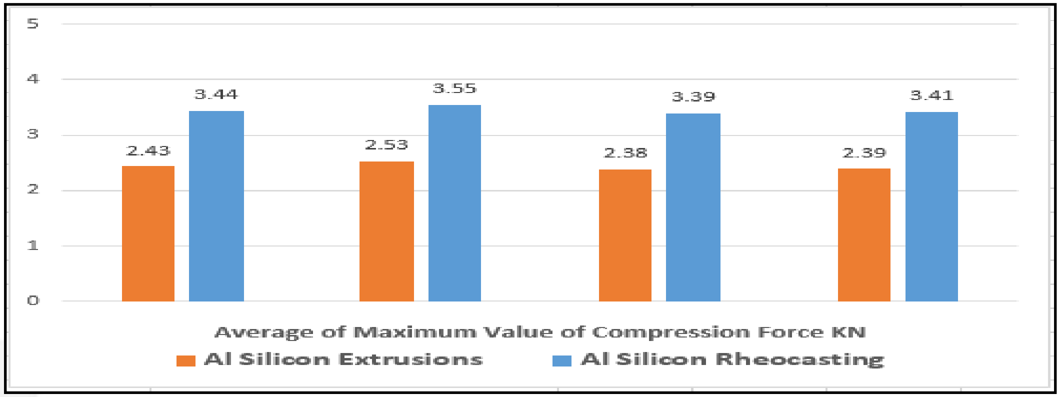

Figure 11. The Maximum Value of Rheocasting alloy and Extrusions alloy Compression Force

The average maximum force for Rheocasting sample was 3.44 KN when the average maximum force for Extrusions sample was 2.43 KN

Previous work

- **Brinell Hardness test**

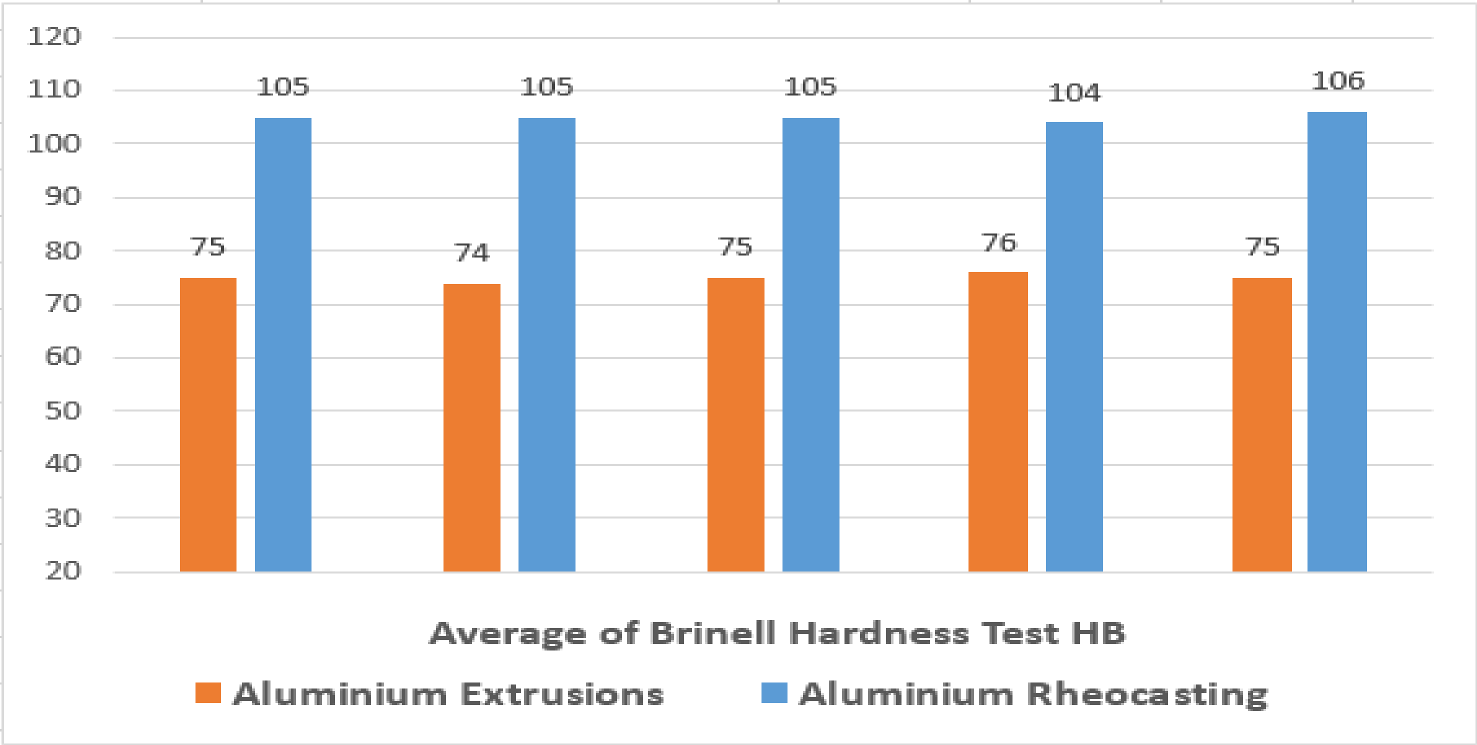

Figure 12. Hardness Brinell of Aluminium EN6063-T6 Extrusions and Rheocasting alloy

The SSR Feedstocks

Aluminum EN AW 6082 alloy

the mold for the impact the samples

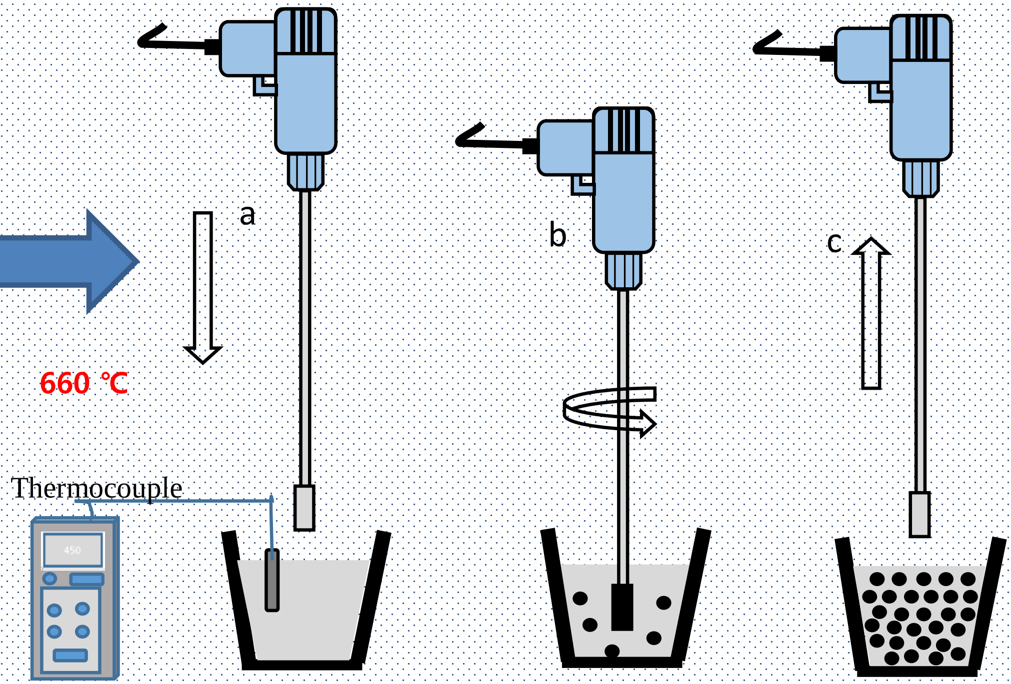

Figure 13. Rheocasting process active in the present work: (a) solid block of the same alloy prepared in advance, attached to a stainless steel rod, (b) dissolved in the melt with simultaneous stirring action, and (c) the slurry thus produced.

Results and Conclusion

- **Impact test**

Figure 14. ACS Compact Test Chambers

Low temperature

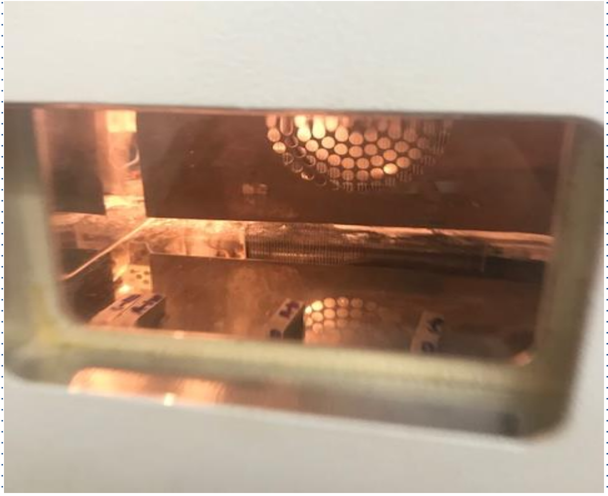

High temperature

Results and Conclusion

- **Impact test**

Rheocasting sample

casting sample

Figure 15. Impact test VEB machine

Figure 16. Charpy Impact test samples a. casting samples b. rheocasting samples

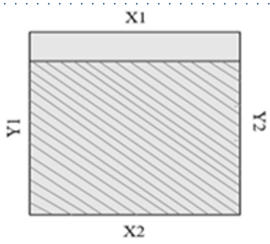

Results and Conclusion

- **Impact test**

standard cross-section area of Charpy impact test

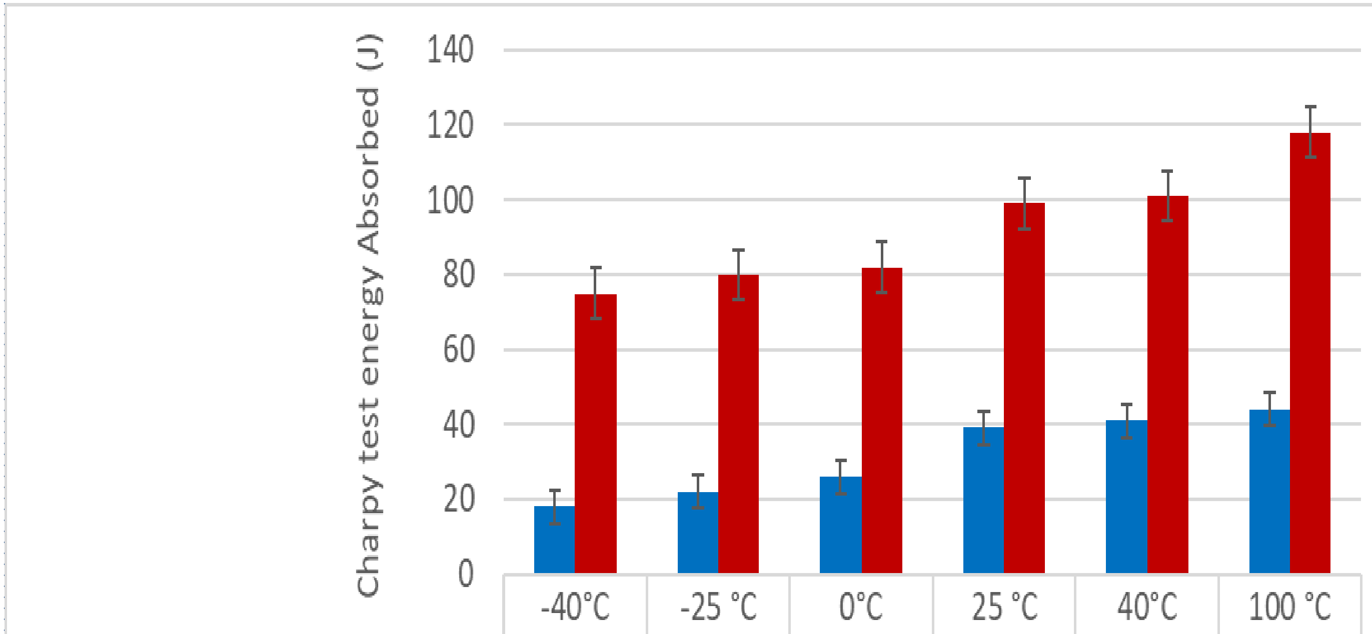

	-40°C	-25 °C	0°C	25 °C	40°C	100 °C
Energy Absorbed (J) For As cast	18	22	26	39	41	44
Energy Absorbed (J) For Rheocasting	75	80	82	99	101	118

Figure 17. the values energy absorbed in casting and rheocasting samples

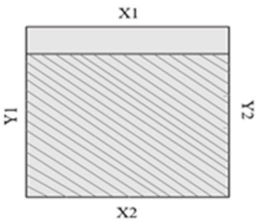

Results and Conclusion

- **Impact test**

standard cross-section area of Charpy impact test

Figure (13) a. Front and side view of as-cast Specimen in 0°C, b. Front and side view of rheocasting Specimen in 0°C

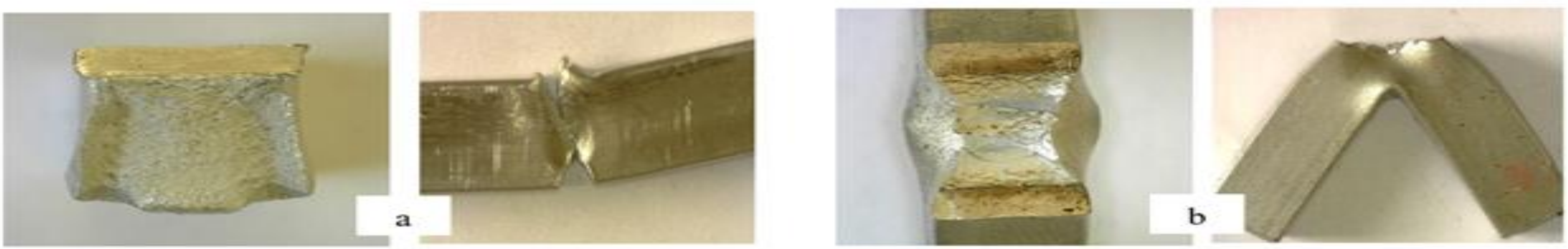

Figure (14) a. Front and side view of as-cast Specimen in 25 °C, b. Front and side view of rheocasting Specimen in 25°C

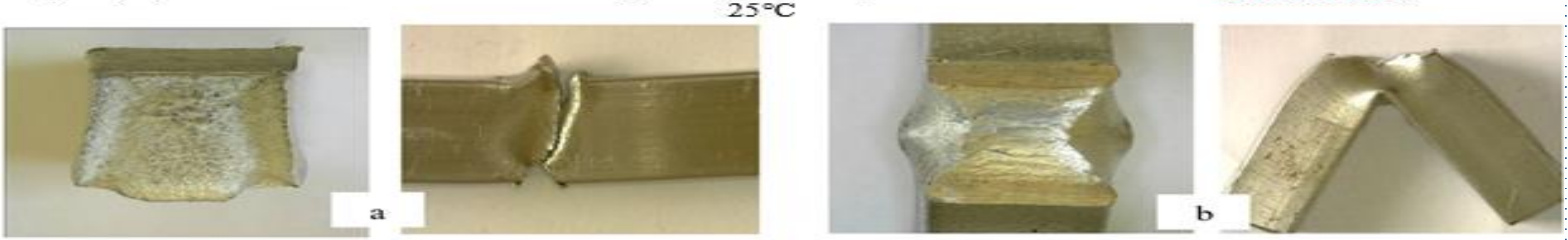

Figure (15) a. Front and side view of as-cast Specimen in 40 °C, b. Front and side view of rheocasting Specimen in 40°C

Figure 18. Measuring the effect Charpy Impact Test in the samples

Results and Conclusion

- **Impact test**

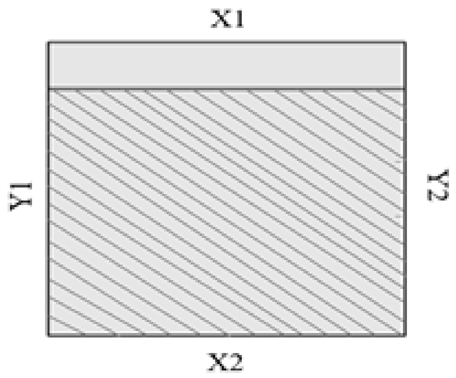

standard cross-section area of Charpy impact test

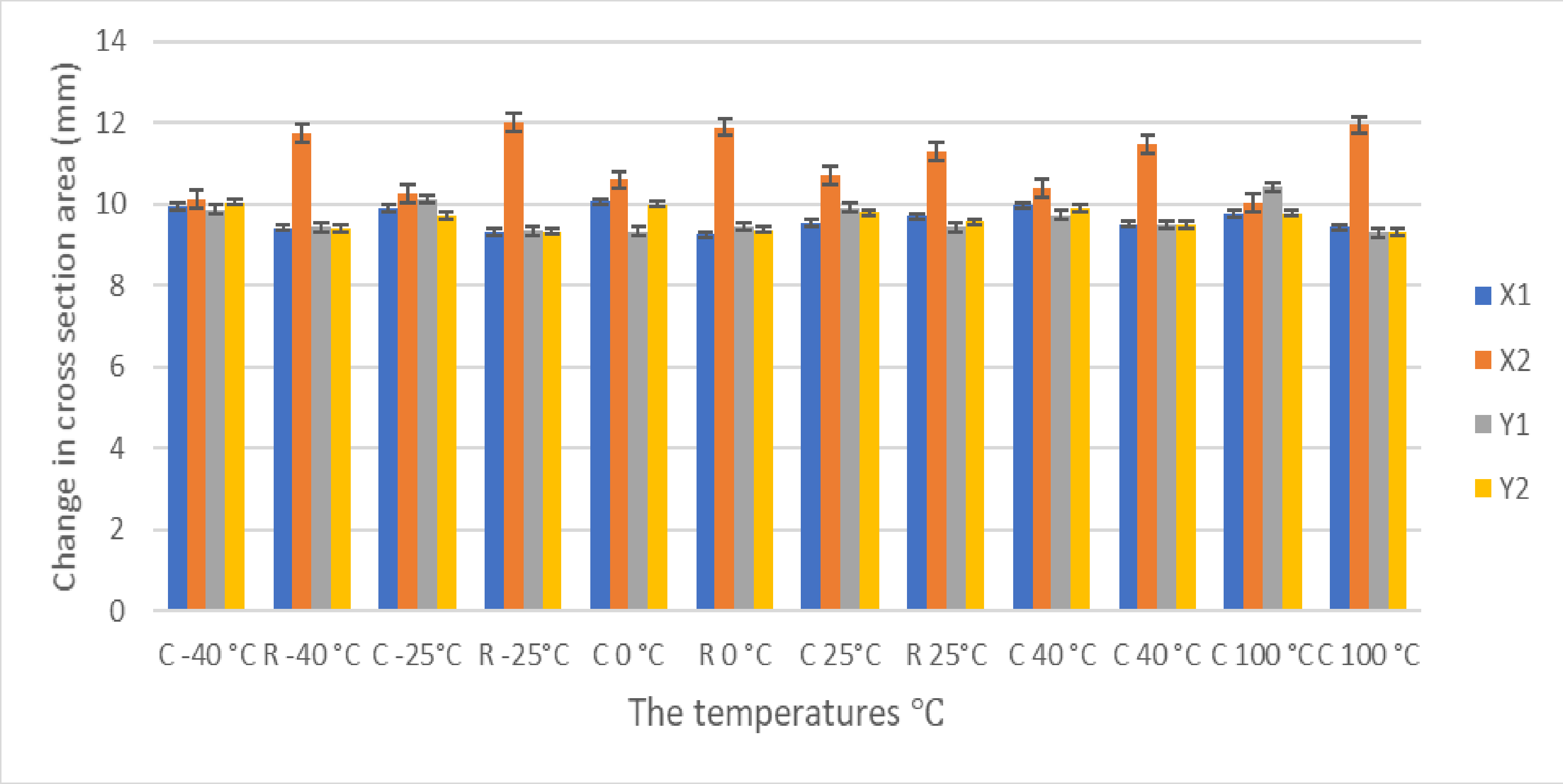

Figure 19. Calculate explosive edge in the Charpy Impact Test

Results and Conclusion

- **Hardness test**

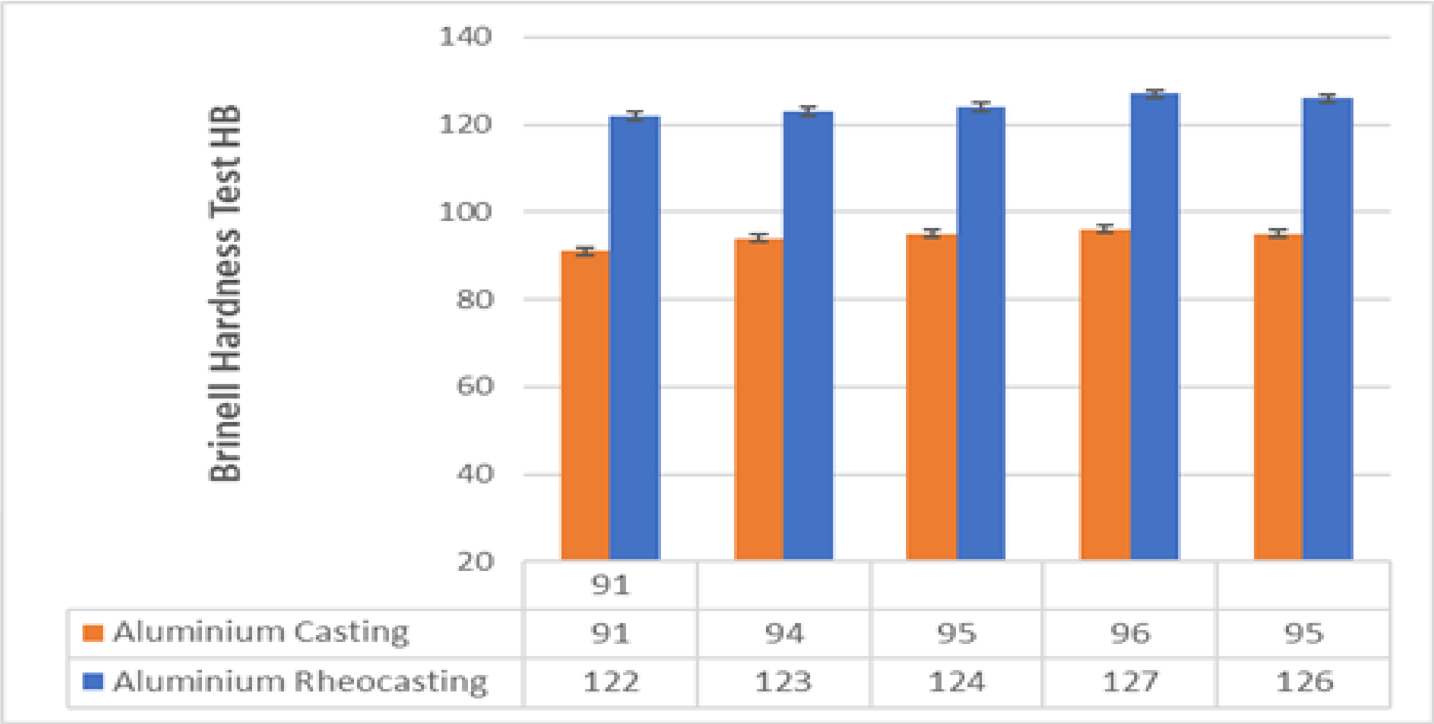

Figure 20. Average hardness Brinell of Aluminium EN AW 6082 and Rheocasting alloy

Results and Conclusion

Scanning Electron Microscope (SEM) for casting and rheocasting samples at room temperature

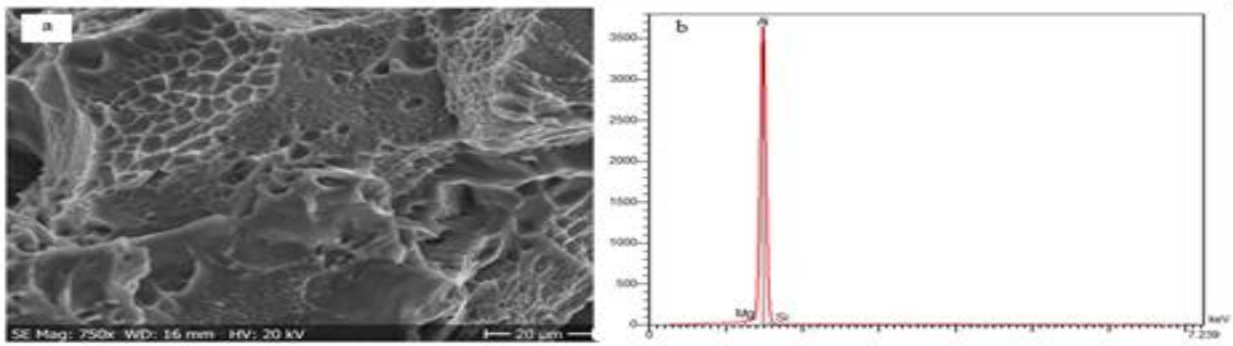

Figure 21. a. The SEM image of grain boundaries in the undeformed part of casting Specimen (39J) b. Energy-dispersive X-ray spectroscopy (EDS) spectrum revealing the precipitation of Mg_2Si of casting Specimen.

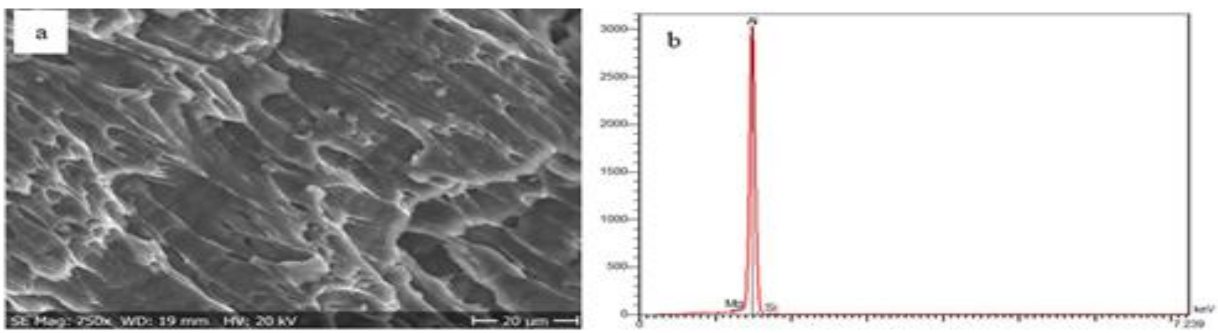

Figure 22. The SEM image of plastic deformation at the grain boundaries of rheocasting Specimen (99J) b. Energy-dispersive X-ray spectroscopy (EDS) spectrum revealing the precipitation of Mg_2Si of rheocasting Specimen.

Activity in all Semesters

Publications

- Publishing paper in International Engineering Symposium at Bánki (IESB 2017) the topic was: (**Comparison of the techniques to produce non-dendritic feedstocks for thixoforming**) (20.11.2017)

- Publishing paper in ***EUROPEAN JOURNAL OF MATERIALS SCIENCE AND ENGINEERING (2019)*** the topic was: (**COMPARISON BETWEEN THE Non-Dendritic Methods of an A201 Aluminum Alloy Depending on Mechanical Properties and Microstructure**) in (02.10.2019)

- Finished work on paper (**Mechanical Properties of Aluminium EN 6063 - T6 Extrusions alloy and Semi-Solid Rheocasting Alloy)**

- Finishing work on paper **(Improvement of Impact toughness Properties for the Rheocasting aluminium alloy EN AW 6082 And Casting aluminium alloy EN AW 6082 In different temperatures**)

Conference Proceedings

- K.A. Abdulrahman, R. Mihály, G. Viktor, **Comparison of the techniques to produce non-dendritic feedstocks for thixoforming**, 9th International Engineering Symposium at Bánki (IESB) (27.11.2017), Budapest, Hungary.

- K.A. Abdulrahman, R. Mihály, G. Viktor, **Evaluation of microstructure and mechanical properties for non-dendritic feedstocks of an EN AW 2011 aluminium allo**y, Smart, Sustainable and Safe Cities Conference (SSSCC) (25.05.2018), Budapest, Hungary.

- K.A. Abdulrahman, R. Mihály, G. Viktor**, Finite Element Modeling Strategies for Semi-Solid Forming**, 10th International Engineering Symposium at Bánki (IESB) (21.11.2018), Budapest, Hungary

Future Research Plan

- **Focusing on the density and porosity of all alloys.**
- **Plane to publishing the two finishing paper .**
- **Start work in my thesis.**

Thanks for your attention!